# Accepted Manuscript

(2*S*)-*N*-2-methoxy-2-phenylethyl-6,7-benzomorphan compound (2*S*-LP2): Discovery of a biased mu/delta opioid receptor agonist

Lorella Pasquinucci, Rita Turnaturi, Girolamo Calò, Francesco Pappalardo, Federica Ferrari, Giulia Russo, Emanuela Arena, Lucia Montenegro, Santina Chiechio, Orazio Prezzavento, Carmela Parenti

Please cite this article as: L. Pasquinucci, R. Turnaturi, G. Calò, F. Pappalardo, F. Ferrari, G. Russo, E. Arena, L. Montenegro, S. Chiechio, O. Prezzavento, C. Parenti, (2*S*)-*N*-2-methoxy-2-phenylethyl-6,7-benzomorphan compound (2*S*-LP2): Discovery of a biased mu/delta opioid receptor agonist, *European Journal of Medicinal Chemistry* (2019), doi: https://doi.org/10.1016/j.ejmech.2019.02.043.

This is a PDF file of an unedited manuscript that has been accepted for publication. As a service to our customers we are providing this early version of the manuscript. The manuscript will undergo copyediting, typesetting, and review of the resulting proof before it is published in its final form. Please note that during the production process errors may be discovered which could affect the content, and all legal disclaimers that apply to the journal pertain.

**(2*S*)-*N*-2-methoxy-2-phenylethyl-6,7-benzomorphan compound (2*S*-LP2): discovery of a biased mu/delta opioid receptor agonist**

Lorella Pasquinucci[a], Rita Turnaturi[a]*, Girolamo Calò[b], Francesco Pappalardo[c], Federica Ferrari[b], Giulia Russo[d], Emanuela Arena[a], Lucia Montenegro[e], Santina Chiechio[c,f], Orazio Prezzavento[a,1] and Carmela Parenti[c,1]


*[a] Department of Drug Sciences, Medicinal Chemistry Section, University of Catania, Viale A. Doria 6, 95125 Catania, Italy*

*[b] Department of Medical Sciences, Pharmacology section, University of Ferrara, via Fossato di Mortara 19, 44121 Ferrara, Italy*

*[c] Department of Drug Sciences, Pharmacology and Toxicology Section, University of Catania, Viale A. Doria 6, 95125 Catania, Italy*

*[d] Department of Biomedical and Biotechnological Sciences, University of Catania, Via Santa Sofia 97, 95125 Catania, Italy*
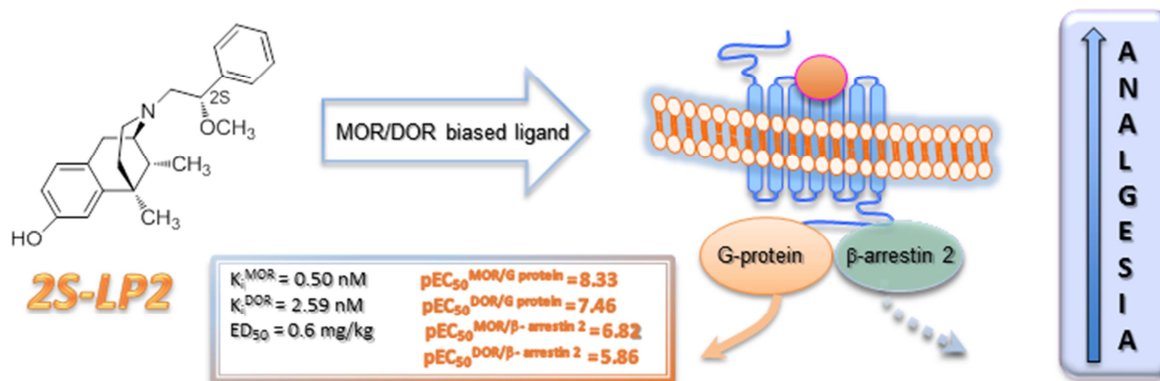
*[e] Department of Drug Sciences, Pharmaceutical Technology Section, University of Catania, Viale A. Doria 6, 95125 Catania, Italy*

*[f] Oasi Research Institute-IRCCS, Troina, Italy*

* Corresponding author.

*E-mail address:* rita.turnaturi@unict.it (Rita Turnaturi)

[1] O.P. and C.P. contributed equally to the work.

**Graphical Abstract**

**Highligthts**

1. The stereocenter role at the *N*-substiyuent of the 6,7-benzomorphan scaffold was investigated.

2. 2*R*- and 2*S*-diastereoisomers of the multitarget opioid ligand LP2 were synthesized.

3. 2*S*-LP2 showed a better pharmacological profile than 2*R*-LP2 in in vitro and in vivo assays.

4. 2*S*-LP2 resulted a biased multitarget MOR/DOR agonist.

5. 2*S*-LP2 elicited an antinociceptive potency 1.5- and 3-times higher than LP2 and *R*-antipode.

**Abstract**

The pivotal role of the stereocenter at the *N*-substituent of the 6,7-benzomorphan scaffold was investigated combining synthetic and pharmacological approaches. 2*R*- and 2*S*-diastereoisomers of the multitarget MOR/DOR antinociceptive ligand LP2 (**1**) were synthesized and their pharmacological profile was evaluated in in vitro and vivo assays. From our results, 2*S*-LP2 (**5**) showed an improved pharmacological profile in comparison to LP2 (**1**) and 2*R*-LP2 (**4**). 2*S*-LP2 (**5**) elicited an antinociceptive effect with a 1.5- and 3-times higher potency than LP2 (**1**) and *R*-antipode (**4**), respectively. In vivo effect of 2*S*-LP2 (**5**) was consistent with the improved MOR/DOR efficacy profile assessed by radioligand binding assay, to evaluate the opioid receptor affinity, and BRET assay, to evaluate the capability to promote receptor/G-protein and receptor/β-arrestin 2 interactions. 2*S*-LP2 (**5**) was able to activate, with different efficacy, G-protein pathway over β-arrestin 2, behaving as biased agonist at MOR and mainly at DOR. Considering the therapeutic potential of both multitarget MOR/DOR agonism and functional selectivity over G-protein, the 2*S*-LP2 (**5**) biased multitarget MOR/DOR agonist could provide a safer treatment opportunity.

**1. Introduction[1]**

Currently used analgesic drugs are chiral compounds often marketed as racemic mixture [1] or single eutomers rather than distomers [2]. For instance, both isomers contribute to the analgesic effect of Tramadol, marketed as mixture 1:1 of 1*R*,2*R*-(+)- and 1*S*,2*S*-(−)-isomers, with a different but complementary mechanism of action [3], while in Nucynta® the pharmacological

---

[1] **SAR,** structure-activity relationship; **MOR**, mu opioid receproe; **DOR**, delta pioid receptor; **GPI**, guinea pig ileum; **MVD**, mouse vas deferens; **BRET**, bioluminescence resonance energy transfer; **KOR**, kappa opioid receptor; **i.p.**, intraperitoneal; **TFL,** tail flick latency.

effect is due to the 1*R*,2*R*-Tapentadol isomer [4]. Thus, drug chirality is assumed to have an important role in both design and development of new analgesic drugs. Despite the fact that isomers share the identical molecular formulas, atom-to-atom linkages, and bonding distances, they are different chemical compounds. Indeed, the isomers could differ in pharmacological, pharmacokinetic and toxicological properties [5] because of the environment of living systems where drug targets are also chiral. Thus, the stereoselective isomer-target interaction could result in different affinity, selectivity and activity, generating substantial differences between isomers [6].

Recently, we synthesized a series of 6,7-benzomorphan-based compounds bearing short and flexible substituents at the basic nitrogen [7]. This SAR study confirmed the importance of *N*-substituent nature in opioid receptors affinity and/or activity modulation. In particular, the increased flexibility of the *N*-substituent and the presence of a hydroxyl or methoxyl group at carbon 2, as hydrogen bond donor and acceptor, allowed an optimal interaction with the opioid receptor binding pocket. Among them, the compound with the (*R/S*)-2-methoxy-2-phenylethyl group as *N*-substituent, named LP2 (**1**, Fig. 1), was characterized by nanomolar affinity for MOR ($K_i$ = 1.08 nM) DOR ($K_i$ = 6.61 nM) and KOR ($K_i$ = 15.22 nM) (Table 1) and in vitro assays (GPI and MVD) LP2 showed MOR/DOR agonist profile ($IC_{50}^{MOR}$ = 21.5 nM and $IC_{50}^{DOR}$ = 4.4 nM). In the tail flick test, after i.p. administration, LP2 produced a long-lasting antinociception, naloxone-reversed, with an $ED_{50}$ of 0.9 mg/kg. Collected data highlighted that LP2 is a multitarget MOR/DOR antinociceptive ligand. Compounds possessing multitarget opioid activity are effective antinociceptive agents with limited adverse effects. In fact, a growing body of evidence [8,9] suggested that in such opioid ligands the additive or synergic antinociceptive

effects coupled with an improved tolerability could be the result of MOR/DOR intermodulatory interactions [10,11].

In the present study, to investigate the role of the stereocenter at the *N*-substituent of the 6,7-benzomorphan scaffold [12,13] in drug-opioid receptor interaction, we evaluated the pharmacological fingerprint of both 2*R*- (**4**) and 2*S*- (**5**) diastereoisomers (Fig. 1) of the multitarget MOR/DOR agonist LP2 (**1**) using a combination of synthetic and pharmacological approaches. To this aim, LP2 diastereoisomers were synthesized. Both diastereoisomers were tested in vitro by competition binding and BRET assays, and in vivo by tail flick test. The pharmacological profile of 2*R*-LP2 (**4**) and 2*S*-LP2 (**5**) were compared each other and with LP2 (**1**).
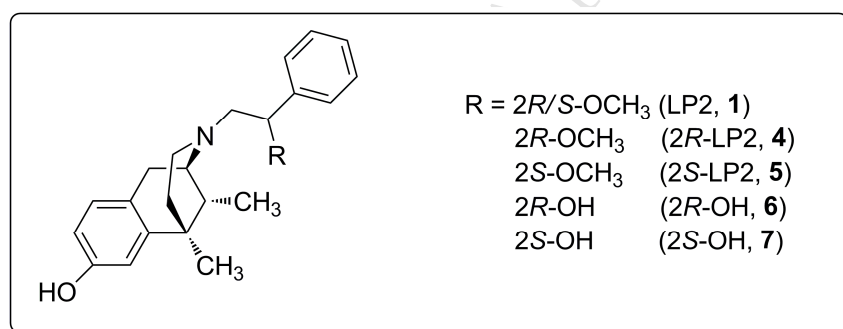


R = 2*R/S*-OCH$_3$ (LP2, **1**)
   2*R*-OCH$_3$   (2*R*-LP2, **4**)
   2*S*-OCH$_3$   (2*S*-LP2, **5**)
   2*R*-OH        (2*R*-OH, **6**)
   2*S*-OH        (2*S*-OH, **7**)

**Fig. 1.** LP2, 2*R*-LP2, 2*S*-LP, 2*R*-OH and 2*S*-OH structures.

## 2. Results and discussion

### 2.1. Chemistry

To obtain compounds 2*R*-LP2 (**4**) and 2*S*-LP2 (**5**), an asymmetric approach was performed as previously reported (Scheme 1) [7]. By means of resolution of commercially available racemic mixture, the (−)-*cis*-*N*-normetazocine was obtained as previously reported [14,15]. Compounds **2** and **3** were prepared by primary alcohol sulfonylation with *p*TsCl and TEA in CH$_2$Cl$_2$ with

catalytic Bu$_2$SnO. Target compounds 2*R*-LP2 (**4**) and 2*S*-LP2 (**5**) were obtained by alkylation of

(–)-*cis-N*-normetazocine with the respective tosylated alcohols **2** and **3**. All compounds were

characterized by $^1$H and $^{13}$C NMR, IR mass spectroscopy and elemental analysis.

**Scheme 1.** Synthetic pathway.
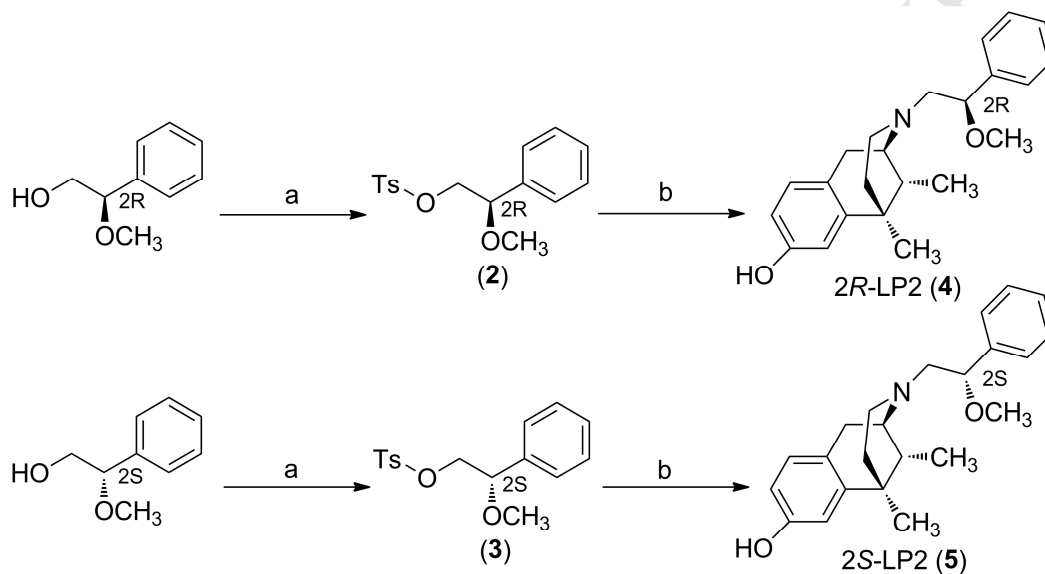


Reagents and conditions: a) TsCl, TEA, Bu$_2$SnO, CH$_2$Cl$_2$, rt, 3 h; b) (-)-*cis-N*-normetazocine, NaHCO$_3$, KI, DMF, 65 °C, 24 h.

*2.2. Radioligand binding assay*

MOR, DOR and KOR binding affinity was determined by radioligand competition binding

experiments on rat or guinea pig brain membranes as previously reported [16]. Inhibition

constant (K$_i$) values, calculated using nonlinear regression analysis (GraphPad Prism, version

5.0), are listed in Table 1.

**Table 1.** Opioid receptor binding affinity of LP2 (**1**), 2*R*-LP2 (**4**) and 2*S*-LP2 (**5**) on rat or guinea pig brain membranes.

| Compd | $K_i$ (nM) ± SEM [a,b] | | | $K_i$ ratio | |
|---|---|---|---|---|---|
| | MOR | DOR | KOR | DOR/MOR | KOR/MOR |
| LP2 (**1**)[c] | 1.08 ± 0.10 | 6.61 ± 0.60 | 15.22 ± 0.80 | 6.11 | 14.10 |
| 2*R*-LP2 (**4**) | 12.30 ± 0.42 | 151.10 ± 0.60 | 236.00 ± 0.83 | 12.28 | 19.20 |
| 2*S*-LP2 (**5**) | 0.50 ± 0.03 | 2.59 ± 0.05 | 26.50 ± 0.44 | 5.18 | 53.00 |
| DAMGO | 1.16 ± 0.10 | - | - | - | - |
| Naltrindole | - | 1.13 ± 0.10 | - | - | - |
| U50,488 | - | - | 0.34 ± 0.10 | - | - |

[a] Values are means ± SEM of three separate experiments, each carried out in duplicate.
[b] $K_i$ values were obtained as [$^3$H]-DAMGO displacement for MOR, [$^3$H]-DPDPE displacement for DOR, and [$^3$H]-(+)-U69,593 displacement for KOR, using nonlinear regression analysis (GraphPad Prism, version 5.0).
[c] Ref. 7

All compounds displayed the capability to inhibit [$^3$H]-DAMGO binding at MOR in a concentration-dependent manner. In comparison to LP2 (**1**), MOR $K_i$ values were 11-times higher for 2*R*-LP2 (**4**) and 2-times lower for the 2*S*-antipode (**5**). 2*R*-LP2 (**4**) DOR affinity was 23-times lower than that of LP2 (**1**). Differently, 2*S*-LP2 (**5**) showed a DOR affinity about 3- and 58-times higher than that of LP2 (**1**) and 2*R*-antipode (**4**), respectively. We also found that KOR affinity of 2*R*-LP2 and 2*S*-LP2 (**4** and **5**) was lower than that of LP2 (**1**). Specifically, 2*S*-LP2 (**5**) KOR affinity resulted 2-times lower, while 2*R*-LP2 (**4**) KOR affinity was 15-times reduced in comparison to the LP2 (**1**) KOR affinity.

The 2-methoxy-2-phenylethyl *N*-substituent of LP2 (**1**) provides a high affinity for MOR and DOR and a moderate affinity for KOR [7]. The results of this study showed that 2*R* configuration (**4**) seemed to be tolerated by MOR but not by DOR and KOR, whereas an improved binding profile at both MOR and DOR was recorded for compound (**5**) with the 2*S*-configuration at the 2-methoxy-2-phenylethyl *N*-substituent.

Previously [7], we reported an analogous trend highlighting the influence of *N*-substituent stereochemistry. Indeed, the 6,7-benzomorphan compound with the 2*S*-hydroxy-2-phenylethyl as *N*-substituent (2*S*-OH, **7**, Figure 1) showed the best MOR ($K_i$= 0.50 ± 0.20 nM), DOR ($K_i$= 0.80 ± 0.20 nM) and KOR ($K_i$= 2.22 ± 0.20 nM) affinity profile, while its 2*R*-antipode (2*R*-OH, **6**, Figure 1) provided MOR, DOR and KOR $K_i$ values 5-, 12- and 3-times higher, respectively.

*2.3. Bioluminescence resonance energy transfer assay*

Based on affinity data and functional selectivity demonstrated by LP2 in GPI versus MOR and MVD versus DOR, the functional activity for MOR and DOR of LP2 (**1**), 2*R*-LP2 (**4**) and 2*S*-LP2 (**5**) was investigated. The compounds were evaluated for their ability to promote receptor/G-protein and receptor/β-arrestin 2 interaction in the BRET assay previously described by Molinari et al. [15]. The results are summarized in Table 2.

**Table 2.** Potencies and efficacies of DADLE, LP2 (**1**), 2*R*-LP2 (**4**) and 2*S*-LP2 (**5**) on MOR/G-protein and MOR/β-arrestin 2 interaction, and DOR/G-protein and DOR/β-arrestin 2 interaction in the BRET assay.

| Compd | $pEC_{50}$ ($CL_{95\%}$) | CR[b] | $\alpha$[c] $\pm$ SEM | $pEC_{50}$ ($CL_{95\%}$) | CR[b] | $\alpha$[c] $\pm$ SEM | Bias factor ($CL_{95\%}$) |
|---|---|---|---|---|---|---|---|
| | **MOR/G-protein** | | | **MOR/β-arrestin 2** | | | |
| DADLE[a] | 6.89 (6.56-7.22) | 1 | 1.00 | 5.86 (5.71-6.01) | 1 | 1.00 | 0 |
| LP2 (**1**) | 7.90 (7.51-8.30) | 0.10 | 0.92 $\pm$ 0.02 | 6.56 (6.22-6.90) | 0.20 | 0.71 $\pm$ 0.09 | 0.57 (0.03-1.16) |
| 2*R*-LP2 (**4**) | crc incomplete[d] | | | inactive | | | - |
| 2*S*-LP2 (**5**) | 8.33 (7.90-8.76) | 0.04 | 0.93 $\pm$ 0.02 | 6.82 (6.43-7.21) | 0.11 | 0.72 $\pm$ 0.08 | 0.82 (0.22-1.41) |
| | **DOR/G-protein** | | | **DOR/β-arrestin 2** | | | |
| DADLE | 7.23 (6.88-7.57) | 1 | 1.00 | 7.69 (7.50-7.87) | 1 | 1.00 | 0 |
| LP2 (**1**) | 7.02 (6.83-7.21) | 2 | 0.96 $\pm$ 0.03 | 5.65 (5.48-5.82) | 110 | 0.90 $\pm$ 0.01 | 2.03 (1.57-2.49) |
| 2*R*-LP2 (**4**) | crc incomplete[d] | | | inactive | | | - |
| 2*S*-LP2 (**5**) | 7.49 (7.24-7.75) | 0.55 | 1.07 $\pm$ 0.03 | 5.73 (5.40-6.07) | 91 | 1.03 $\pm$ 0.03 | 2.31 (1.84-2.77) |

[a] DADLE was used as reference agonist for calculating intrinsic activity at the MOR and DOR.
[b] CR is the ratio between $EC_{50}$ of tested compounds and $EC_{50}$ of standard agonist (DADLE).
[c] $\alpha$ is the ratio between the intrinsic activity of tested compounds and intrinsic activity of standard agonist (DADLE) as maximal-stimulated BRET ratio ($\alpha = 1$).
[d] Crc incomplete means that maximal effects could not be determined due to the low potency of the compound.
Data are the mean $\pm$ SEM of at least 5 separate experiments made in duplicate.

9

Membrane extracts taken from SH-SY5Y cells stably co-expressing the MOR/RLuc and Gβ1/RGFP fusoproteins were used in concentration-response experiments to evaluate receptor/G-protein interaction. DADLE promoted MOR/G-protein interaction in a concentration-dependent manner with potency of 6.89 and maximal effect of $0.81 \pm 0.10$ stimulated BRET ratio (Fig. 2, panel A).
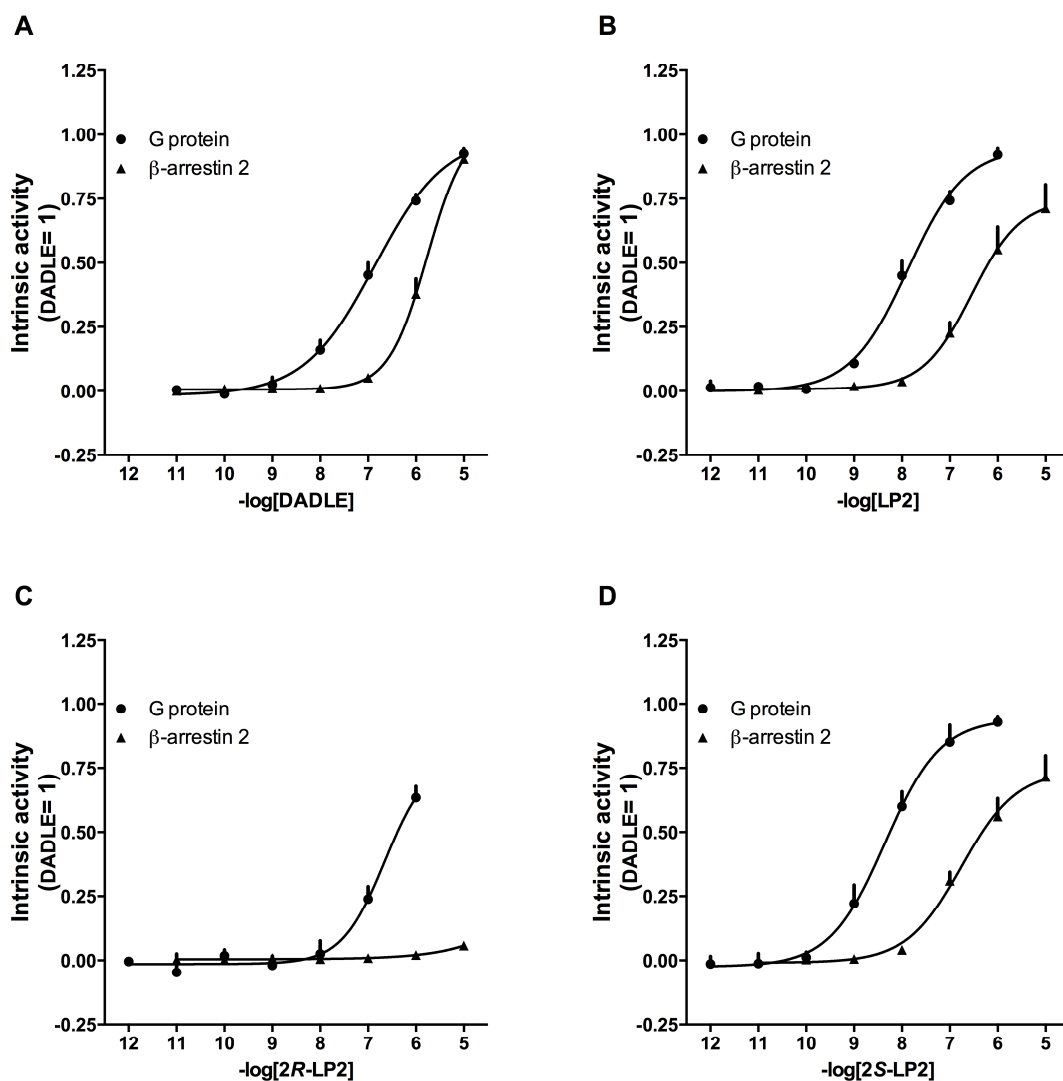
**A**



**B**

**C**

**D**

**Fig. 2.** Concentration-response curve to DADLE (panel A), LP2 (**1**, panel B), 2*R*-LP2 (**4**, panel C) and 2*S*-LP2 (**5**, panel D) in promoting MOR/G-protein and MOR/β-arrestin 2 interaction. Data are the mean $\pm$ SEM of 5 separate experiments made in duplicate.

The intrinsic activities of tested compounds were computed as fraction of DADLE maximal-stimulated BRET ratio ($\alpha = 1$). LP2 (**1**) and 2$S$-LP2 (**5**) (Fig. 2, panel B and D) mimicked the maximal effect of DADLE ($pEC_{50} = 6.93$) being 10- and 30-times more potent ($pEC_{50} = 8.06$ and 8.33, respectively). Compound 2$R$-LP2 (**4**) was able to elicit a weakly stimulatory response only at the highest concentration tested (Fig. 2, panel C).

Whole SH-SY5Y cells stably expressing the MOR/RLuc and the $\beta$-arrestin 2/RGFP fusoproteins were used to evaluate MOR/$\beta$-arrestin 2 interaction. DADLE stimulated the interaction of the MOR with $\beta$-arrestin 2 in a concentration-dependent manner with $pEC_{50}$ of 5.86 and maximal effects corresponding to $0.57 \pm 0.20$ stimulated BRET ratio (Fig. 2, panel A). As for G-protein studies, the intrinsic activities of the compounds were computed as fraction of the standard agonist DADLE. Compounds LP2 (**1**) and 2$S$-LP2 (**5**) mimicked the stimulatory response of DADLE with slightly lower efficacy but 5- and 9-times higher potency, respectively (Fig. 2, panel B and C). 2$R$-LP2 (**4**) was inactive (Fig. 2, panel C). The results showed in Fig. 2 were used for calculating the bias factor of the ligands: LP2 (**1**) and 2$S$-LP2 (**5**) displayed a modest (<10 times) bias toward G-protein that reached the statistical level of significance only for the latter compound (Table 2).

In SH-SY5Y cells stably co-expressing the DOR/RLuc and the G$\beta$1/RGFP fusoproteins, DADLE promoted receptor/G-protein interaction in a concentration-dependent manner displaying a $pEC_{50}$ value of 7.23 and maximal effect of $0.42 \pm 0.04$ stimulated BRET ratio (Fig. 3, panel A). The intrinsic activities of tested compounds were computed as fraction of DADLE maximal-stimulated BRET ratio ($\alpha = 1$).
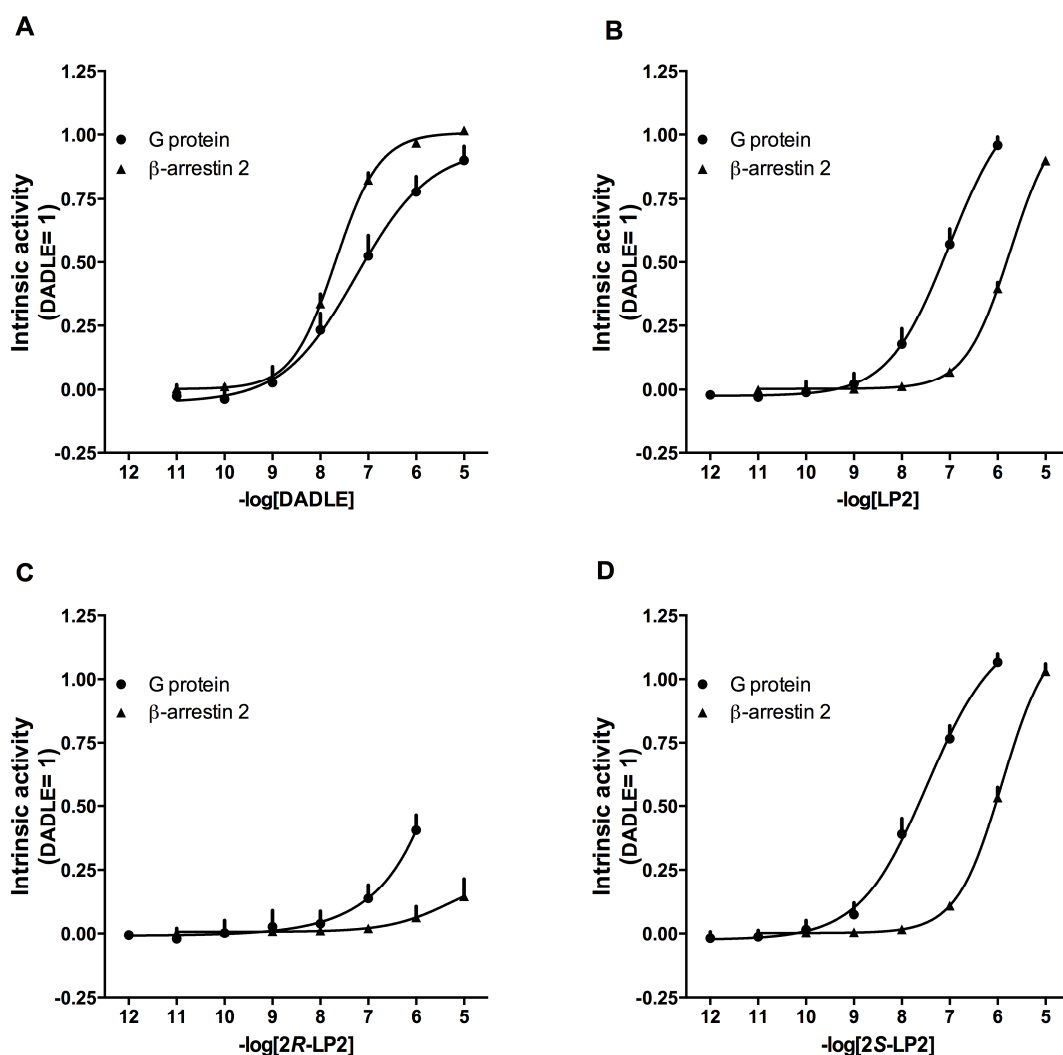
**Fig. 3.** Concentration response curve to DADLE (panel A), LP2 (**1**, panel B), 2*R*-LP2 (**4**, panel C) and 2*S*-LP2 (**5**, panel D) in promoting DOR/G-protein and DOR/β-arrestin 2 interaction. Data are the mean ± SEM of 7 separate experiments made in duplicate.

In parallel experiments, LP2 (**1**) and 2*S*-LP2 (**5**) (Fig. 3, panel B and D) behaved as full agonists with similar potency and similar efficacy as the standard (Table 2). Compound 2*R*-LP2 (**4**) was able to elicit a weakly stimulatory response only at the highest concentration tested (Figure 3, panel C).

Whole SH-SY5Y cells stably co-expressing the DOR/RLuc and the β-arrestin 2/RGFP fusoproteins were used to evaluate DOR/β-arrestin 2 interaction. DADLE

stimulated the interaction of the DOR with β-arrestin 2 in a concentration-dependent manner with $pEC_{50}$ of 7.69 and maximal effects corresponding to $0.47 \pm 0.05$ stimulated BRET ratio (Fig. 3, panel A). The intrinsic activities of the compounds under study were computed as fraction of DADLE. LP2 (**1**) and 2*S*-LP2 (**5**) mimicked the maximal effects of DADLE being, however, less potent (Fig. 3, panel B and D), while 2*R*-LP2 (**4**) was inactive (Fig. 3, panel C). Fig. 3 showed the comparison of the effects of each compound on the DOR/G-protein and DOR/β-arrestin 2 interaction. These results were used for calculating the bias factor of LP2 (**1**) and 2*S*-LP2 (**5**); both compounds showed a statistically significant and large (200-times) bias toward G-protein (Table 2).

Figure 4 shows the bias factors for LP2 (**1**) and 2*S*-LP2 (**5**) at MOR and DOR between G-protein and β-arrestin 2 recruitment.
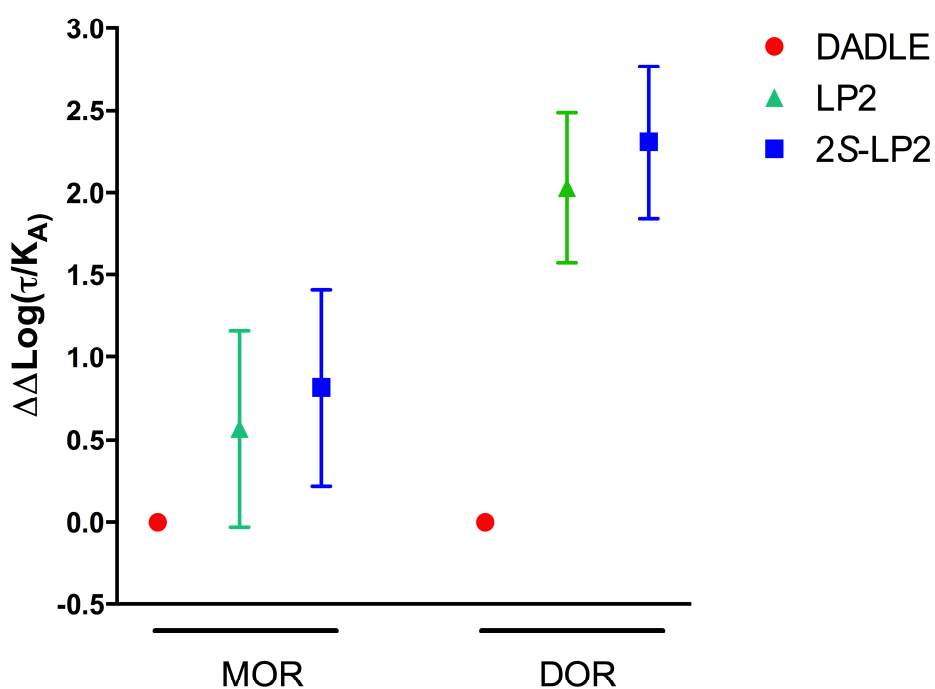


**Fig. 4.** Bias factor (mean $\pm$ $CL_{95\%}$) of LP2 (**1**) and 2S-LP2 (**5**) toward G-protein and β-arrestin 2. DADLE was used as reference agonist for both receptors.

We used BRET assay to examine the capability to promote MOR and DOR/G-protein interaction of the previously synthesized 6,7-benzomorphans with 2$R$-OH (**6**) and 2$S$-OH (**7**, Fig. S1) [7] to compare the role of the chirality. Similarly, 2$S$-OH (**7**) showed the best MOR/DOR agonist profile (pEC$_{50}^{MOR}$ = 8.18, α = 0.87 and pEC$_{50}^{DOR}$ = 7.84, α = 1.13) in comparison with the 2$R$-OH (**6**) (pEC$_{50}^{MOR}$ = 7.65, α = 0.82 and pEC$_{50}^{DOR}$ = 7.23, α = 1.03) (Table S1).

After binding at MOR and DOR, LP2 (**1**) and 2$S$-LP2 (**5**) are able to activate, with different efficacy, G-protein pathway over β-arrestin 2, behaving as biased agonist at MOR and mainly at DOR. It has been demonstrated that the G-protein pathway induces analgesia, while the β-arrestin pathway is responsible for the opioid-related adverse reactions [18,19]. Recently, G-protein biased opioid agonists were identified and the relationship between in vitro bias profile and in vivo analgesia and side effects were highlighted [20-22]. Thus, the 2$S$-LP2 (**5**) biased multitarget MOR/DOR agonist could provide a safer treatment opportunity.

*2.4. Tail Flick Test*

The antinociceptive effect of 2$R$-LP2 (**4**) and 2$S$-LP2 (**5**), i.p. administered, was examined using mouse tail-flick test [23]. Both compounds produced a dose-dependent analgesic effect compared to the group of mice treated with saline (*p< 0.05 vs saline-treated mice).

In comparison to LP2 (**1**), featured by a maximal antinociceptive threshold reached between 45 and 60 min after injection and a prolonged analgesic effect with an ED$_{50}$ of 0.9 mg/kg [7], both isomers showed different onset and duration of the antinociceptive effect and different ED$_{50}$. In vivo evaluation of 2$R$-LP2 (**4**) established that the maximal antinociceptive activity was reached 60 min after i.p. injection and lasted over 120 min after treatment (Fig. 5, panel A). Moreover, 2$R$-

14

isomer (**4**) showed the antinociceptive effect at higher doses with an $ED_{50}$ of 1.8 mg/kg i.p. (1.2-2.8, $CL_{95\%}$) (Fig. 5, panel B).
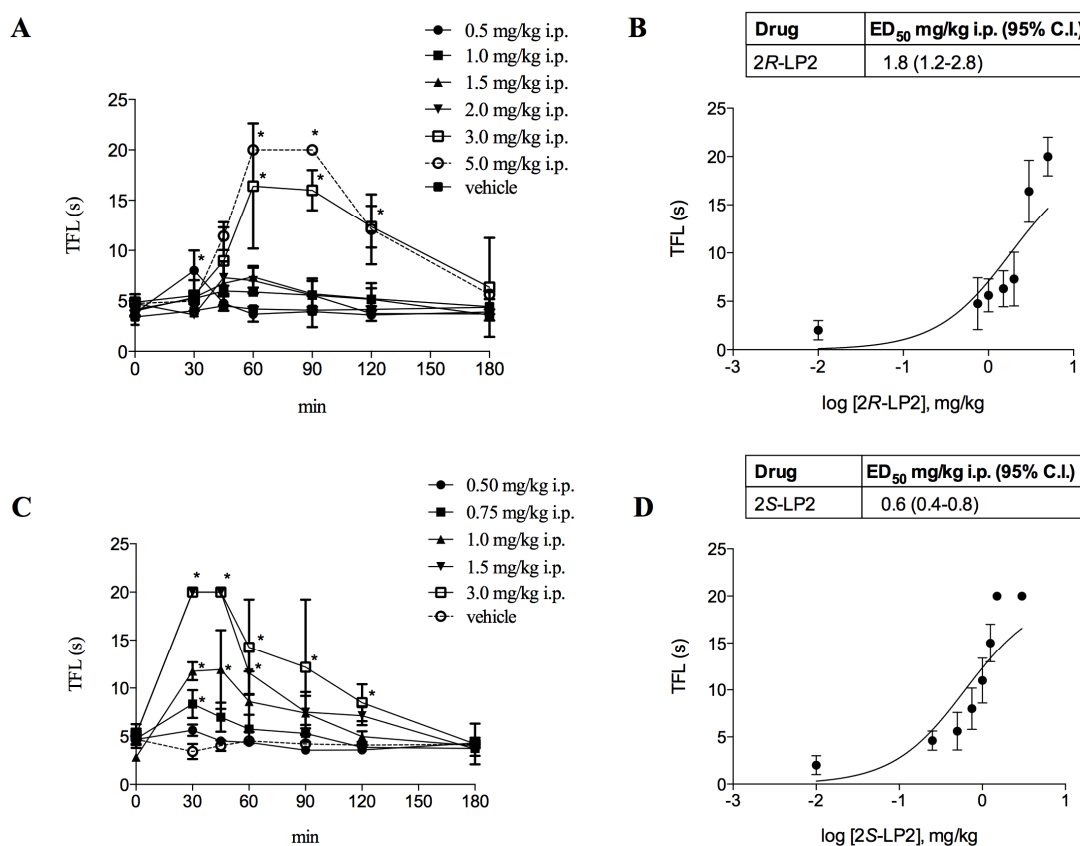


**Fig. 5.** (A) Time-course (min) of 2*R*-LP2 (**4**) induced antinociception measured by TFL. (B) Analgesic dose-response curve ± SEM for compound 2*R*-LP2 (**4**) was plotted at 60 min post-treatment. (C) Time-course (min) of 2*S*-LP2 (**5**) induced antinociception measured by TFL. (D) Analgesic dose-response curve ± SEM for compound 2*S*-LP2 (**5**) was plotted at 30 min post-treatment. Results are expressed in seconds (s). Data are means ± SEM from 6 to 8 mice. *$p < 0.05$ vs saline-treated mice.

A robust antinociceptive effect was achieved at very low doses of 2*S*-LP2 (**5**), with an $ED_{50}$ of 0.6 mg/kg i.p. (0.4-0.8, CL95%) (Fig. 5, panel D), that revealed its highest effect already at 30 min post-administration (Fig. 5, panel C). At the tested doses, 2*R*-LP2 (**4**) and 2*S*-LP2 (**5**) didn't affect significantly behavior responses (i.e. locomotor activity and sedation; unpublished data).

15

Therefore, 2$R$-LP2 (**4**) and 2$S$-LP2 (**5**) exhibited a different profile in modulating acute thermal nociception. The more potent activity of 2$S$-LP2 (**5**) translated the MOR/DOR affinity (binding assay) and the full MOR/DOR agonist activity (BRET assay) into the behavioral antinociceptive assay. Therefore, in vivo results confirmed that $S$-configuration of $N$-substituent improved the pharmacological profile in comparison with 2$R$-isomer (**4**). We demonstrated the same trend for 6,7-benzomorphan 2$S$-OH (**7**) that showed an $ED_{50}$ of 1.0 mg/kg i.p. (0.7-1.5, $CL_{95\%}$) better than the 2$R$-isomer (2$R$-OH, **6**) with an $ED_{50}$ of 1.3 mg/kg i.p. (0.9-2.1, $CL_{95\%}$) [7].

2$R$-LP2 (**4**) in vivo profile does not reflect in vitro data. Indeed, 2$R$-LP2 (**4**) exhibited only 3-times difference in antinociceptive efficacy than 2$S$-LP2 (**5**) but about 25-times less affinity for MOR, and about 58-times less affinity for DOR, resulting a very weak agonist at MOR and inactive at DOR. This behavior could be due to 2$R$-LP2 (**4**) pharmacokinetic properties or stability [1,2,24].

**3. Conclusion**

The pivotal role of the stereocenter at the $N$-substituent of the 6,7-benzomorphan scaffold was pointed out combining synthetic and pharmacological approaches. It is well known that the stereochemistry could affect pharmacological parameters such as potency, intrinsic efficacy and binding affinity in ligand-opioid receptor interaction. The development of a single isomer in place of a previous racemic mixture, a process known as "chiral switching", could provide potential advantages such as an improved therapeutic index, decreased side-effects, a faster onset of action and a reduced liability for drug-drug interactions [25].

2$R$-(**4**) and 2$S$-LP2 (**5**) were featured by a qualitatively similar but quantitatively different pharmacological fingerprint in agreement with the importance of

16

stereoselective drug-opioid receptor interaction. Specifically, 2*S*-LP2 (**5**) showed an antinociceptive effect at a very low dose with potency 1.5- and 3-times increased in comparison to LP2 (**1**) and *R*-antipode (**4**), respectively. The in vivo effect of 2*S*-LP2 (**5**) was consistent with its MOR and DOR affinity profile combined to the improved multitarget MOR/DOR full agonist profile. Moreover, 2*S*-LP2 (**5**) resulted a biased MOR/DOR agonist. It has been demonstrated that biased opioid ligands selectively activate G-protein signalling leading to more effective antinociceptive drugs with fewer side effects. Such biased ligands could have a major impact on modern drug discovery and represent a new strategy for the development of more tolerated drug candidates [26,27]. Indeed, their functional selectivity for G-protein signalling and reduced β-arrestin 2 recruitment could be consistent with their effectiveness in chronic pain conditions management [28,29]. Thus, the advantageous pharmacological profile of 2*S*-LP2 (**5**) could be the result of its capability to simultaneously target MOR and DOR, that it has been widely demonstrated to be a valid strategy to obtain an improved antinociceptive effect coupled with an improved tolerability, combined with its capability to selectively promote the G-protein signalling.

**4. Experimental section**

*4.1. Chemistry*

*4.1.1. General methods*

General methods are reported in Supporting Information. All reported compounds had a purity of at least 95%.

*4.1.2. General procedure for the synthesis of tosylate intermediates (2-3)*

17

The synthesis of tosylate intermediates **2**-**3** was performed as previously reported [7] using (*R*)-(−)-2-methoxy-2-phenylethanol or (*S*)-(+)-2-methoxy-2-phenylethanol (see Supporting Information).

*4.1.2.1. (R)-2-methoxy-2-phenylethyl 4-methylbenzenesulfonate (**2**).* Waxy solid (94%). Mp: 52-55 °C. $[\alpha]_D^{25}$ = − 42.9° (c 1.05, CHCl$_3$). IR (CHCl$_3$) 3019, 2943, 1598, 1456, 1362, 1215, 1176 cm$^{-1}$. $^1$H NMR (200 MHz, CDCl$_3$): δ 7.76-7.72 (m, 2H, CH Ts), 7.32-7.26 (m, 7H, CH Ts and aryl), 4.42-4.39 (m, 1H, CH-O), 4.09-4.03 (m, 2H, CH$_2$), 3.23-3.20 (t, 3H, -OCH$_3$), 2.44 (s, 3H, CH$_3$). $^{13}$C NMR (50 MHz, CDCl$_3$) δ 144.79, 136.63, 132.91, 129.69, 128.62, 128.55, 127.83, 126.85, 81.15, 72.79, 56.98, 21.46 (see Supporting Information Figure S2-S4).

.

*4.1.2.2. (S)-2-methoxy-2-phenylethyl 4-methylbenzenesulfonate (**3**).* Waxy solid (74%). Mp 54-55 °C. $[\alpha]_D^{25}$ = + 42.2° (c 1.02, CHCl$_3$). IR (CHCl$_3$) 3019, 2934, 1598, 1455, 1361, 1215, 1176 cm$^{-1}$. $^1$H NMR (200 MHz, CHCl$_3$) δ 7.76-7.72 (m, 2H, CH Ts), 7.43-7.22 (m, 7H, CH Ts and aryl), 4.44-4.39 (m, 1H, CH-O) 4.09-4.03 (m, 2H, CH$_2$), 3.23-3.21 (t, 3H, -OCH$_3$), 2.44 (s, 3H, CH$_3$). $^{13}$C NMR (50 MHz, CHDl$_3$) δ 144.67, 136.73, 132.92, 129.72, 128.65, 128.57, 127.86, 126.88, 81.12, 72.85, 57.01, 21.59. (see Supporting Information Figure S5-S7).

*4.1.3. General procedure for the synthesis of N-Substituted (−)-cis-N-normetazocine diastereomers (**4**-**5**)*

Compounds **4**-**5** were obtained as previously reported [7] (see Supporting Information).

*4.1.3.1.* *(2R,6R,11R)-3-((R)-2-methoxy-2-phenylethyl)-6,11-dimethyl-1,2,3,4,5,6-hexahydro-2,6-methanobenzo[d]azocin-8-ol (4).* White solid (62 %). Mp 176-180 °C. $[\alpha]_D^{25} = -53.7°$ (c 1.05, EtOH). $^1$H NMR (200 MHz, CDCl$_3$, free base) δ 7.32-7.19 (m, 5H, CH aryl), 6.83 (d, 1H, *J* = 8.2 Hz, CH benzomorphan), 6.65 (d, 1H, *J* = 2.2 Hz, CH benzomorphan), 6.55 (dd, 1H, *J* = 8.2, 2.2 Hz, CH benzomorphan), 4.35 (d, 1H, CH-O), 3.13 (s, 3H, -OCH$_3$), 2.89-2.55 (m, 6H, CH, CH$_2$ benzomorphan and CH$_2$), 2.23-2.11 (m, 1H, CH benzomorphan), 1.90-1.82 (m, 2H, CH$_2$ benzomorphan), 1.24 (s, 3H, CH$_3$ benzomorphan), 1.18-1.10 (m, 1H, CH benzomorphan), 0.73 (d, 3H, CH$_3$ benzomorphan). $^{13}$C NMR (50 MHz, CDCl$_3$, free base) δ 154.29, 143.05, 141.07, 128.33, 128.11, 127.66, 127.50, 126.66, 113.06, 112.32, 81.68, 62.12, 58.7, 56.60, 46.74, 41.12, 40.33, 36.06, 25.29, 23.89, 14.11(see Supporting Information Figure S8-S9). MS m/z [M]$^+$ 351.4. Anal (C$_{23}$H$_{29}$NO$_2$·HCl) C, H, N (see Supporting Information Table S2).

*4.1.3.2.* *(2R,6R,11R)-3-((S)-2-methoxy-2-phenylethyl)-6,11-dimethyl-1,2,3,4,5,6-hexahydro-2,6-methanobenzo[d]azocin-8-ol (5).* White solid (60 %). Mp 177-180 °C; $[\alpha]_D^{25} = +68.3°$ (c 1.05, EtOH). $^1$H NMR (200 MHz, CDCl$_3$, free base) δ 7.25-7.19 (m, 5H, CH aryl), 6.83 (d, 2H, *J* = 8.2 Hz, CH benzomorphan), 6.65 (d, 1H, *J* = 2.0 Hz, CH benzomorphan), 6.55 (dd, 1H, *J* = 8.2, 2.2 Hz, CH benzomorphan), 4.42 (d, 1H, CH-O), 3.15 (s, 3H, -OCH$_3$), 2.97-2.55 (m, 6H, CH, CH$_2$ benzomorphan and CH$_2$), 2.11-1.85 (m, 3H, CH and CH$_2$ benzomorphan), 1.25 (s, 3H, CH$_3$ benzomorphan), 1.18-1.15 (m, 1H, CH benzomorphan), 0.76 (m, 3H, CH$_3$ benzomorphan). $^{13}$C NMR (50 MHz, CDCl$_3$, free base) δ 154.51, 142.79, 140.55, 128.43, 128.15, 127.86, 127.76, 126.57, 113.16, 112.25, 81.61, 61.88, 58.79, 56.71, 46.02, 41.05, 40.31, 35.91, 25.18, 24.05, 14.01(see Supporting Information Figure

S10-S11). MS m/z $[M]^+$ 351.4. Anal ($C_{23}H_{29}NO_2 \cdot HCl$) C, H, N (see Supporting Information Table S2).

## 4.2. Receptor binding assays

### 4.2.1. Drugs and reagents

Radioligands $[^3H]$-DAMGO, $[^3H]$-DPDPE and $[^3H]$-(+)-U69,593 were purchased by Perkin-Elmer Life Sciences (Boston, MA, USA). Naloxone hydrochloride was purchased from Tocris Bioscience (Bristol, United Kingdom).

### 4.2.2. Competitive Radioligand Binding Assay

MOR, DOR and KOR binding experiments were performed on rat or guinea pig brain membranes according to the experimental protocol described by Spetea et al. [30] without modifications, as reported elsewhere [31]. Protein concentration was determined by Lowry's method using bovine serum albumin as standard [32]. Binding experiments at MOR and DOR were carried out by incubating 0.4 mg/mL and 0.5 mg/mL of rat brain membrane proteins, respectively for 45 min at 35 °C either with 1 nM $[^3H]$-DAMGO (48.4 Ci/mM) or 2 nM $[^3H]$-DPDPE (52.7 Ci/mM) in 50 mM Tris-HCl (pH 7.4). Regarding KOR binding assays, guinea pig brain membranes (0.5 mg/mL) were incubated for 30 min at 30 °C with 1 nM $[^3H]$-(+)-U69,593 (42.69 Ci/mM). Test compounds were added in concentration ranging from $10^{-5}$ to $10^{-11}$ M. Nonspecific binding was assessed in the presence of 10 μM of unlabeled naloxone. The reaction was terminated by filtering the solution through Whatman GF/B glass fiber filters, which were presoaked for 1h in a 0.5% polyethylenimine solution. Filters were washed with ice cold buffer (2×4 mL), dried, soaked in 4 mL of "Ultima Gold MV" scintillation cocktail and counted on a Beckman LS 6500 liquid scintillation counter.

### 4.2.3. Data analysis

$K_i$ values were calculated using nonlinear regression analysis to fit a logistic equation to the competition data using GraphPad Prism version 5.0 (GraphPad Software In., San Diego, USA).

### 4.3. Functional assay

### 4.3.1. Drugs and reagents

All cell culture media and supplements were from Invitrogen (Thermo Fisher Scientific Inc. MA, USA). All other reagents were from Sigma Chemical Co. (Poole, U.K.) and were of the highest purity available. DADLE was from Sigma Chemical Co. (Poole, U.K.), DADLE was solubilized in bidistilled water, while compounds **1**, **4** and **5** were solubilized in DMSO (5% v/v) at a final concentration of 10 mM. Stock solutions of ligands were stored at -20 °C.

### 4.3.2. BRET assay

SH-SY5Y cells were grown in Dulbecco's modified Eagle's medium (DMEM)/HAMS F12 (1:1) supplemented with 10% fetal bovine serum, penicillin G (100 units/mL), streptomycin (100 µg/mL), L-glutamine (2 mM), fungizone (1 µg/mL), geneticin (G418; 400 µg/mL) and hygromycin B (100 µg/mL) in a humidified atmosphere of 5% $CO_2$ at 37 °C. Cell lines permanently co-expressing the different pairs of fusion proteins (MOR-RLuc/Gβ1-RGFP, MOR-RLuc/β-arrestin 2-RGFP, DOR-RLuc/Gβ1-RGFP, and DOR-RLuc/β-arrestin 2-RGFP) were prepared using the pantropic retroviral expression system by Clontech as described previously [33]. For G-protein experiments enriched plasma membrane aliquots from transfected cells were prepared by differential centrifugation; cells were detached with PBS/EDTA solution (1 mM, pH 7.4 NaOH) then, after 5 min 500 g centrifugation,

Dounce-homogenized (30 strokes) in cold homogenization buffer (Tris 5 mM, EGTA 1 mM, DTT 1 mM, pH 7.4 HCl) in the presence of sucrose (0.32 M). Three following centrifugations were performed at 10 min 1000 g (4 °C) and the supernatants kept. Two 20 min 24,000 g (4 °C) subsequent centrifugations (the second in the absence of sucrose) were performed for separating enriched membranes that after discarding the supernatant were kept in ultrapure water at -80 °C [34]. The protein concentration in membrane preparations was determined using the QPRO-BCA kit (Cyanagen Srl, Bologna, IT) and the spectrophotometer Ensight (Perkin Elmer, Waltham, US).

Luminescence in membranes and cells was recorded in 96-well white opaque microplates (PerkinElmer, Waltham, MA, USA) using the luminometer Victor 2030 (PerkinElmer, Waltham, MA, USA). For the determination of receptor/G-protein interaction, membranes (3 μg of protein) prepared from cells co-expressing MOR-RLuc/Gβ1-RGFP or DOR-RLuc/Gβ1-RGFP were added to wells in DPBS. For the determination of receptor/β-arrestin 2 interaction, cells co-expressing MOR-RLuc/β-arrestin 2-RGFP or DOR-RLuc/β-arrestin 2-RGFP were plated 24h before the experiment (100,000 cells/well). The cells were prepared for the experiment substituting the medium with PBS with $MgCl_2$ (0.5 mM) and $CaCl_2$ (0.9 mM). Coelenterazine at a final concentration of 5 μM was injected 15 minutes prior reading the cell plate. Different concentrations of ligands in 20 μL of PBS - BSA 0.01 % were added and incubated 5 min before reading luminescence. All the experiments were performed at room temperature.

### 4.3.3. Data analysis and terminology

The pharmacological terminology adopted in this paper were consistent with IUPHAR recommendations [35]. All data were expressed as the mean ± standard error of the mean (SEM of n experiments). For potency values 95% confidence limits

22

(CL$_{95\%}$) were indicated. BRET data were calculated as BRET ratio between CPS measured for the RGFP and RLuc light emitted using 510(10) and 460(25) filters (PerkinElmer, Waltham, MA, USA), respectively. Maximal agonist effects were expressed as fraction of the DADLE maximal effects that was determined in every assay plate. Agonist potencies were given as pEC$_{50}$ i.e. the negative logarithm to base 10 of the molar concentration of an agonist that produces 50% of the maximal effect of that agonist. Concentration-response curves to agonists were fitted to the classical four-parameter logistic nonlinear regression model:

$$\text{Effect} = \text{baseline} + \frac{E_{\max} - \text{baseline}}{1 + 10^{(\text{LogEC}_{50} - \text{Log}_{[\text{compound}]})\text{Hillslope}}}$$

Curve fitting was performed using PRISM 6.0 (GraphPad Software In., San Diego, USA). pEC$_{50}$ was the concentration of agonist producing a 50% maximal response and n was the Hill coefficient of the concentration-response curve to the agonist. CR was the ratio between EC$_{50}$ of ligand and EC$_{50}$ of standard agonist (DADLE). Maximal effects have been statistically analyzed with one-way ANOVA followed by the Dunnett's post hoc test for multiple comparisons; P values less than 0.05 were considered statistically significant.

Bias factors were calculated by choosing DADLE as standard unbiased ligand. The concentration response curves of each compound were fitted to the Black-Leff operational model described by Nagi & Pineyro [36]:

$$response = \frac{[A^n]\tau^n E_m}{[A]^n\tau^n + ([A] + K_A)^n}$$

where [A] is the agonist concentration, the maximal response of the system is given by $E_m$, *n* is a fitting parameter for the slope, the affinity of the agonist is represented by the equilibrium dissociation constant of the agonist-receptor complex ($K_A$), and the efficacy of the agonist is defined by $\tau$. $\tau$ and $K_A$ are descriptive parameters of intrinsic

efficacy and binding affinity and may be directly obtained by fitting experimental data to the operational equation and can be expressed as "transduction coefficients" $\log(\tau/K_A)$. The relative efficiency of agonists producing activation of any pathways can thus be quantified with a "normalized" transduction coefficient, namely $\Delta\log(\tau/K_A)$. Finally, the bias factors were calculated as difference between $\Delta\log(\tau/K_A)$ values for a given agonist between the pathways (G protein and β-arrestin 2):

$$\Delta\Delta\log(\tau/KA) \text{ (bias factor)} = \Delta\log(\tau/K_A)_{G \text{ protein}} - \Delta\log(\tau/K_A)_{\beta\text{-arrestin } 2}$$

Bias factors are expressed as the mean ± SEM of at least 5 independent experiments.

*4.4. In vivo pharmacology*

*4.4.1. Animals*

Male Swiss CB1 mice (Envigo Laboratories, S.Pietro al Natisone (UD)) weighing 25-30 g were housed six to a cage. Animals were kept at a constant room temperature (25 ± 1 °C) under a 12:12h light and dark cycle with free access to food and water. Each mouse was used for only one experiment. Experimental procedures were approved by the Local Ethical Committee (IACUC) and conducted in accordance with international guidelines as well as European Communities Council Directive and National Regulations (CEE Council 86/609 and DL 116/92).

*4.4.2. Nociceptive Test*

Nociception was evaluated by the radiant heat tail-flick test [37,38]. Briefly, it consisted of irradiation of the lower third of the tail with an infrared source (Ugo Basile, Comerio, Italy). The day before the experiment, mice were habituated to the procedure for measuring nociception threshold. Experiments were performed at room temperature (25 ± 1 °C). The basal pre-drug latency was established between 3 and 5 s and was calculated as the average of the first three measurements, which were

performed at 5 min intervals. A cutoff latency of 20 s was established to minimize damage to the tail. All tested compounds were dissolved in pyrogen-free isotonic saline (Baxter Healthcare, Deerfield, IL) and DMSO (5%) and were administered to mice i.p. Post-treatment tail flick latencies (TFLs) were determined at 30, 60, 90, 120, 150 and 180 min after i.p. injection.

### 4.4.2. Statistical Analysis

All values were presented as means ± SD. Intergroup comparisons were assessed using an initial two-way analysis of variance (ANOVA) followed by Duncan's multiple range post-hoc test. Differences were considered significant when $*p < 0.05$. Effective dose-50 ($ED_{50}$) values were calculated using least-squares linear regression analysis followed by calculation of 95% confidence limits ($CL_{95\%}$) by the method of Bliss [39,40].

### Conflicts of interest

The authors declare no other conflicts of interest.

### Acknowledgements

### Appendix A. Supplementary data

Supplementary data related to this article can be found at

### References

[1] J. Gal, Molecular chirality: language, history, and significance, Top. Curr. Chem. 340 (2013) 1–20, DOI: 10.1007/128_2013_435.

[2] N. Chhabra, M. L. Aseri, D. Padmanabhan, A review of drug isomerism and its significance, Int. J. Appl. Basic Med. Res. 3 (2013) 16–18, DOI: 10.4103/2229-516X.112233.

[3] L. Bravo, J.A. Mico, E. Berrocoso, Discovery and development of tramadol for the treatment of pain, Expert Opin. Drug Discov. 12 (2017) 1281–1291, DOI: 10.1080/17460441.2017.1377697.

[4] N. Vadivelu, D. Chang, E.M. Helander, G.J. Bordelon, A. Kai, A.D. Kaye, D. Hsu, D. Bang, I. Julka, Ketorolac, Oxymorphone, Tapentadol, and Tramadol: A Comprehensive Review, Anesthesiol. Clin. 35 (2017) e1–e20, DOI: 10.1016/j.anclin.2017.01.001.

[5] S.W. Smith, Chiral toxicology: it's the same thing...only different, Toxicol. Sci. 110 (2009) 4-30, DOI: 10.1093/toxsci/kfp097.

[6] J. McConathy, M.J. Owens, Stereochemistry in Drug Action, Prim. Care Companion J. Clin. Psychiatry 5 (2003) 70–73, DOI: 10.4088/PCC.v05n0202.

[7] L. Pasquinucci, R. Turnaturi, O. Prezzavento, E. Arena, G. Aricò, Z. Georgoussi, R. Parenti, G. Cantarella, C. Parenti, Development of novel LP1-based analogues with enhanced delta opioid receptor profile, Bioorg. Med. Chem. 25 (2017) 4745–4752, DOI: 10.1016/j.bmc.2017.07.021.

[8] R. Turnaturi, G. Aricò, G. Ronsisvalle, C. Parenti, L. Pasquinucci, Multitarget opioid ligands in pain relief: New players in an old game, Eur. J. Med. Chem. 108 (2016) 211–228, DOI: 10.1016/j.ejmech.2015.11.028.

[9] L. Pasquinucci, R. Turnaturi, L. Montenegro, F. Caraci, S. Chiechio, C. Parenti. Simultaneous targeting of MOR/DOR: A useful strategy for inflammatory pain modulation. Eur. J. Pharmacol. 847 (2019) 97–102. doi: 10.1016/j.ejphar.2019.01.031..

[10] E.B. Margolis, W. Fujita, L.A. Devi, H.L. Fields, Two delta opioid receptor subtypes interact with the mu opioid receptor, Neuropharmacology 123 (2017) 420–432, DOI: 10.1016/j.neuropharm.2017.06.019.

[11] C.M. Cahill, E. Ong, Evidence and function relevance of native DOR-MOR heteromers, in: Handb. Exp. Pharmacol. Springer, Berlin, Heidelberg, 2018, pp. 1–13, DOI: 10.1007/164_2018_112.

[12] R. Turnaturi, A. Marrazzo, C. Parenti, L. Pasquinucci, Benzomorphan scaffold for opioid analgesics and pharmacological tools development: A comprehensive review, Eur. J. Med. Chem. 148 (2018) 410–422, DOI: 10.1016/j.ejmech.2018.02.046.

[13] R. Turnaturi, L. Montenegro, A. Marrazzo, R. Parenti, L. Pasquinucci, C. Parenti, Benzomorphan skeleton, a versatile scaffold for different targets: A comprehensive review, Eur. J. Med. Chem. 155 (2018) 492–502. DOI: 10.1016/j.ejmech.2018.06.017.

[14] L. Pasquinucci, C. Parenti, E. Amata, Z. Georgoussi, P. Pallaki, V. Camarda, G. Calò, E. Arena, L. Montenegro, R. Turnaturi, Synthesis and Structure-Activity Relationships of (-)-cis-N-Normetazocine-Based LP1 Derivatives, Pharmaceuticals. 11 (2018) pii: E40. doi: 10.3390/ph11020040.

[15] R. Turnaturi, C. Parenti, O. Prezzavento, A. Marrazzo, P. Pallaki, Z. Georgoussi, E. Amata, L. Pasquinucci, Synthesis and Structure-Activity Relationships of LP1 Derivatives: N-Methyl-N-phenylethylamino Analogues as Novel MOR Agonists, Molecules 23 (2018) E677, DOI: 10.3390/molecules23030677.

[16] L. Pasquinucci, O. Prezzavento, A. Marrazzo, E. Amata, S. Ronsisvalle, Z. Georgoussi, D.D. Fourla, G.M. Scoto, C. Parenti, G. Aricò, G. Ronsisvalle,

Evaluation of N-substitution in 6,7-benzomorphan compounds, Bioorg. Med. Chem. 18 (2010) 4975–4982, DOI: 10.1016/j.bmc.2010.06.005.

[17] P. Molinari, V. Vezzi, M. Sbraccia, C. Gro, D. Riitano, C. Ambrosio, I. Casella, T. Costa, Morphine-like opiates selectively antagonize receptor-arrestin interactions, J. Biol. Chem. 285 (2010) 12522−12535, DOI: 10.1074/jbc.M109.059410.

[18] H. Bu, X. Liu, X. Tian, H. Yang, F. Gao, Enhancement of morphine analgesia and prevention of morphine tolerance by downregulation of β-arrestin 2 with antigene RNAs in mice, Int. J. Neurosci. 125 (2015) 56−65. DOI: 10.3109/00207454.2014.896913.

[19] Y. Li, X. Liu, C. Liu, J. Kang, J. Yang, G. Pei, C. Wu, Improvement of morphine-mediated analgesia by inhibition of β-arrestin2 expression in mice periaqueductal gray matter, Int. J. Mol. Sci. 10 (2009) 954−963. DOI: 10.3390/ijms10030954.

[20] J.D. Violin, A.L. Crombie, D.G. Soergel, M.W. Lark, Biased ligands at G-protein-coupled receptors: promise and progress, Trends Pharmacol. Sci. 35 (2014) 308–316, DOI: 10.1016/j.tips.2014.04.007.

[21] N. Audet, I; Charfi, O. Mnie-Filali, M. Amraei, A.J. Chabot-Doré, M. Millecamps, L.S. Stone, G. Pineyro, Differential association of receptor-Gβγ complexes with β-arrestin2 determines recycling bias and potential for tolerance of δ opioid receptor agonists, J. Neurosci. 32 (2012) 4827–4840, DOI: 10.1523/JNEUROSCI.3734-11.2012.

[22] C.L. Schmid, N.M. Kennedy, N.C. Ross, K.M. Lovell, Z. Yue, J. Morgenweck, M.D. Cameron, T.D. Bannister, L.M. Bohn, Bias Factor and Therapeutic Window Correlate to Predict Safer Opioid Analgesics, Cell. 171 (2017) 1165-1175. DOI: 10.1016/j.cell.2017.10.035.

[23] L. Pasquinucci, R. Turnaturi, G. Aricò, C. Parenti, P. Pallaki, Z. Georgoussi, S. Ronsisvalle, Evaluation of N-substituent structural variations in opioid receptor profile of LP1, Bioorg. Med. Chem. 24 (2016) 2832–2842, DOI: 10.1016/j.bmc.2016.05.005.

[24] A. Rubin, M.P. Knadler, P.P. Ho, L.D. Bechtol, R.L. Wolen, Stereoselective inversion of (R)-fenoprofen to (S)-fenoprofen in humans, J. Pharm. Sci. 74 (1985) 82–84, DOI: 10.1002/jps.2600740122.

[25] A. Calcaterra, I. D'Acquarica, The market of chiral drugs: Chiral switches versus de novo enantiomerically pure compounds, J. Pharm. Biomed. Anal. 147 (2018) 323–340, DOI: 10.1016/j.jpba.2017.07.008.

[26] S. Majumdar, LA. Devi, Strategy for making safer opioids bolstered, Nature 553 (2018) 286–288, DOI: 10.1038/d41586-018-00045-1.

[27] Kennedy, NM; Schmid, CL; Ross, NC; Lovell, KM; Yue, Z; Chen, YT; Cameron, MD; Bohn, LM; Bannister, TD. Optimization of a Series of Mu Opioid Receptor (MOR) Agonists with High G Protein Signaling Bias. J. Med. Chem. 61 (2018) 8895–8907, DOI: 10.1021/acs.jmedchem.8b01136.

[28] M. Koblish, R. Carr 3rd, E.R. Siuda, D.H. Rominger, W. Gowen-MacDonald, C.L. Cowan, A.L. Crombie, J.D. Violin, MW. Lark, TRV0109101, a G Protein-Biased Agonist of the μ-Opioid Receptor, Does Not Promote Opioid-Induced Mechanical Allodynia following Chronic Administration, J. Pharmacol. Exp. Ther. 362 (2017) 254–262, DOI: 10.1124/jpet.117.241117.

[29] A. Bedini, S.M. Spampinato, Innovative Opioid Peptides and Biased Agonism: Novel Avenues for More Effective and Safer Analgesics to Treat Chronic Pain, Curr. Med. Chem. (2017) 1–22. DOI: 10.2174/0929867324666170216095233.

[30] M. Spetea, C.R. Bohotin, M.F. Asim, K. Stübegger, H. Schmidhammer, In vitro and in vivo pharmacological profile of the 5-benzyl analogue of 14-methoxymetopon, a novel mu opioid analgesic with reduced propensity to alter motor function, Eur. J. Pharm. Sci. 41 (2010) 125–135, DOI: 10.1016/j.ejps.2010.05.018.

[31] O. Prezzavento, E. Arena, C. Sánchez-Fernández, R. Turnaturi, C. Parenti, A. Marrazzo, R. Catalano, E. Amata, L. Pasquinucci, E.J. Cobos, (+)-and (−)-Phenazocine enantiomers: Evaluation of their dual opioid agonist/σ(1) antagonist properties and antinociceptive effects, Eur. J. Med. Chem. 125 (2017) 603–610, DOI: 10.1016/j.ejmech.2016.09.077.

[32] O.H. Lowry, N.J. Rosebrough, A.L. Farr, R.J. Randall, Protein measurement with the folin phenol reagent, J. Biol. Chem. 193 (1951) 265–275.

[33] D. Malfacini, C. Ambrosio, M.C. Gro, M. Sbraccia, C. Trapella, R. Guerrini, M. Bonora, P. Pinton, T. Costa, G. Calo', Pharmacological Profile of Nociceptin/Orphanin FQ Receptors Interacting with G-Proteins and beta-Arrestins 2, PloS one 10 (2015) e0132865, DOI: 10.1371/journal.pone.0132865.

[34] L. Vachon, T. Costa, A. Herz, Opioid receptor desensitization in NG 108-15 cells. Differential effects of a full and a partial agonist on the opioid-dependent GTPase, Biochem. Pharmacol. 36 (1987) 2889–2897, DOI: 10.1016/0006-2952(87)90199-7.

[35] R. R. Neubig, M. Spedding, T. Kenakin, A. Christopoulos, International Union of Pharmacology Committee on Receptor Nomenclature and Drug Classification. International Union of Pharmacology Committee on Receptor Nomenclature and Drug Classification. XXXVIII. Update on terms and symbols in quantitative pharmacology, Pharmacol Rev. 55 (2003) 597–606, DOI: 10.1124/pr.55.4.4.

[36] K. Nagi, G. Pineyro, Practical guide for calculating and representing biased signaling by GPCR ligands: A stepwise approach, Methods 92 (2016) 78−86, DOI: 10.1016/j.ymeth.2015.09.010.

[37] M.L. Accolla, R. Turnaturi, M.G. Sarpietro, S. Ronsisvalle, F. Castelli, L. Pasquinucci, Differential scanning calorimetry approach to investigate the transfer of the multitarget opioid analgesic LP1 to biomembrane model, Eur. J. Med. Chem. 77 (2014) 84−90, DOI: 10.1016/j.ejmech.2014.02.056.

[38] L. Pasquinucci, C. Parenti, R. Turnaturi, G. Aricò, A. Marrazzo, O. Prezzavento, S. Ronsisvalle, Z. Georgoussi, D.D. Fourla, G.M. Scoto, G. Ronsisvalle, The benzomorphan-based LP1 ligand is a suitable MOR/DOR agonist for chronic pain treatment, Life Sci. 90 (2012) 66−70, DOI: 10.1016/j.lfs.2011.10.024.

[39] C. Parenti, R. Turnaturi, G. Aricò, A. Marrazzo, O. Prezzavento, S. Ronsisvalle, G.M. Scoto, G. Ronsisvalle, L. Pasquinucci, Antinociceptive profile of LP1, a non-peptide multitarget opioid ligand, Life Sci. 90 (2012) 957−961, DOI: 10.1016/j.lfs.2012.04.041.

[40] C.I. Bliss, Statistics in Biology. New York, NY: McGraw-Hill, 1967; pp 558−639.

**Highlights**

1.  The stereocenter role at the *N*-substituent of the 6,7-benzomorphan scaffold was investigated.

2.  2*R*- and 2*S*-diastereoisomers of the multitarget opioid ligand LP2 were synthesized.

3.  2*S*-LP2 showed a better pharmacological profile than 2*R*-LP2 in in vitro and in vivo assays.

4.  2*S*-LP2 resulted a biased multitarget MOR/DOR agonist.

5.  2*S*-LP2 elicited an antinociceptive potency 1.5- and 3-times higher than LP2 and *R*-antipode.